

# Towards a mid-infrared SWIFTS: L-band integrated high resolution spectrometer

Myriam Bonduelle<sup>a</sup>, Guillermo Martin<sup>a</sup>, Salma Baccar<sup>a,b</sup>, Noémie Mestre<sup>a,b</sup>, Alain Morand<sup>b</sup>, Víctor Arroyo Heras<sup>c</sup>, Javier R. Vázquez de Aldana<sup>c</sup>, Carolina Romero<sup>c</sup>, Nadège Courjal<sup>d</sup>, Roland Salut<sup>d</sup>, and Laurent Robert<sup>d</sup>

<sup>a</sup>Univ. Grenoble Alpes, CNRS, IPAG, 38000 Grenoble, France

<sup>b</sup>Univ. Grenoble Alpes, Univ. Savoie Mont Blanc, CNRS, Grenoble INP\*, CROMA, 38000 Grenoble, France \*Institute of Engineering Univ. Grenoble Alpes

<sup>c</sup>Grupo de Investigación en Aplicaciones del Láser y Fotónica (ALF-USAL), Facultad de Ciencias, Universidad de Salamanca, E-37008 Salamanca, Spain

<sup>d</sup>FEMTO-ST, Univ. Franche-Comté, 25030 Besançon, France

## ABSTRACT

This work aims to present the first results towards a mid-infrared (L-band : 3.4  $\mu\text{m}$  - 4.1  $\mu\text{m}$ ) high resolution integrated spectrometer, based on the Gabor approach of SWIFTS (Stationary Wave Integrated Fourier Transform Spectrometer). In this configuration, a stationary wave is obtained by injecting the light from the source on both sides of a channel waveguide. The centre of the coherent interferogram is obtained in the middle of the waveguide, allowing for full characterisation of the source, and all differential dispersion effects between the two optical paths. The stationary wave is sampled by nano-scattering centres (= nanogrooves) placed on top of the waveguide. They extract the interferogram, and the spectrum of the source is retrieved through a Fourier Transform. In the mid-infrared, the detection area of the detectors is buried : using only one groove per scattering centre leads to a diffracted signal too wide and causes pixel crosstalk. Several grooves per scattering centres have therefore been implemented, as this configuration creates a small diffraction grating, and reduces the angular divergence of the flux. In addition to avoiding crosstalk, this allows to extract more flux per scattering centre, thus increasing the signal to noise ratio. Our samples are made in Lithium Niobate (LiNbO<sub>3</sub>), an electro-optic crystal, using two technologies. First, Direct Laser Writing for both the waveguides and the nanogrooves, and secondly Titane diffusion for the waveguides and Focused Ion Beam for the nanogrooves. Because of the electro-optic properties of Lithium Niobate, applying an electric field ramp modulation will change the refractive index of the material, allowing to finely scan the fringe packet under the sampling centres, thus increasing the sampling rate of the interferogram by temporal multiplexing. We demonstrate that our waveguides are fully functional and have a correct transmission rate, and that our antennas are extracting the stationary wave as expected, in both technologies.

**Keywords:** Astrophotonics, Spectroscopy, L-band, Lithium Niobate, Integrated Optics, Miniature spectrometer, Ultrafast Laser Writing, Titane Diffusion

## 1. INTRODUCTION

Spectrometers, that allow the study of the spectrum of a chosen source, are used in multiple domains (astrophysics,<sup>1</sup> environmental monitoring.<sup>2</sup>). Although bulk spectrometers offer unparalleled resolution over wide spectral ranges they are usually voluminous and costly instruments. Newer applications (satellite monitoring, space missions, in-situ measurements...) are calling for smaller, more cost efficient spectrometers, paving the way to the development of miniature integrated spectrometers.<sup>3</sup>

We are here presenting the building blocks for the implementation of a L-band (3.4  $\mu\text{m}$  to 4.1  $\mu\text{m}$ ) SWIFTS,<sup>4</sup> a miniature integrated spectrometer.

---

Corresponding author: Myriam Bonduelle

E-mail: myriam.bonduelle@univ-grenoble-alpes.fr

## 2. SWIFTS PRINCIPLE

The principle behind the SWIFTS spectrometer is to sample a stationary wave created in a channel waveguide through the use of nano-scattering centres placed on top of the considered waveguide. The configuration that presented here is a Gabor configuration, where the wave is obtained by injecting the light on both sides of the waveguide, creating an interferogram in the middle of the waveguide. This interferogram is then sampled by dielectric discontinuities: in this work grooves etched in the material, that will sample the evanescent part of the wave. A complete SWIFTS, not presented here, will have a detector directly glued onto the sample, so as to avoid any relay optics.

Finally, the spectrum of the source is retrieved through a Fourier Transform.

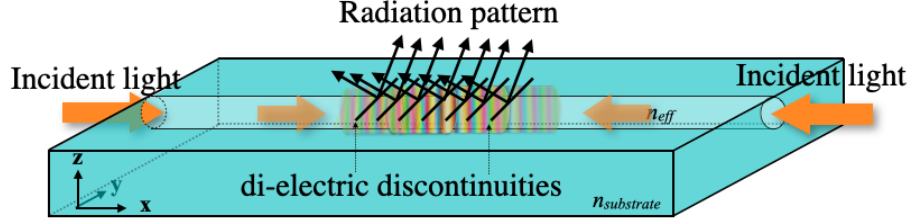


Figure 1: Principle of a SWIFTS Gabor: the light is injected on both sides of the waveguide, creating an interferogram with an optical path difference of 0 in the middle of the waveguide, that is extracted by the scattering centres (= grooves).

The resolution of a SWIFTS is given by:<sup>4</sup>

$$R = \frac{\lambda}{\Delta\lambda} = \frac{2n_{eff} \cdot L}{\lambda} \quad (1)$$

with  $n_{eff}$  the effective refractive index in the waveguide,  $\lambda$  the considered wavelength, and  $L$  the sampled length. In the case of the studied sample, at a wavelength of 3.4  $\mu\text{m}$ , a sampled length of 1 cm will result in a resolution over 10 000 ( $\Delta\lambda \sim 340$  pm).

The spectral bandwidth of a SWIFTS is characterised by:<sup>4</sup>

$$\Delta\lambda_{bandwidth} = \frac{\lambda^2}{4n_{eff}\Lambda} \quad (2)$$

with  $\Lambda$  the pitch between two consecutive scattering centres. This value of  $\Lambda$  cannot be below the characteristic pixel pitch in MIR detectors: this would result in crosstalk, and the impossibility to correctly reconstruct the interferogram -and therefore spectrum- of the source. With a 30  $\mu\text{m}$  pixel size, the spectral bandwidth of this SWIFTS configuration is 44 nm.

With those characteristics, a mid-IR SWIFTS is a high resolution miniature spectrometer, but with a very restrained bandwidth. In order to improve this bandwidth, spatial multiplexing,<sup>5</sup> or temporal multiplexing can be considered. In the case of this sample, the latter has been implemented, through the choice of the material. All of the samples were made in Lithium Niobate ( $\text{LiNbO}_3$ ), a bi-refrigrant crystal that shows a Pockels effect. This implies that the application of an electric field onto the sample will locally change the refractive index of the material, resulting in the possibility to shift the fringe packet under the sampling centres, effectively reducing the pitch between two consecutive centres. The variation  $\Delta n_{EO}$  can be expressed as a function of the applied electric field through:

$$\Delta n_{EO} = -\frac{1}{2} \cdot n^3 \cdot r_{51} \cdot E_{app} \quad (3)$$

with  $n$  the refractive index of Lithium Niobate,  $r_{51}$  an electro-optic coefficient specific to lithium niobate (around a few dozens pm/V), and  $E_{app}$  the applied electric field.

### 3. FABRICATION METHODS

Implementing a functional SWIFTS requires to firstly obtain single-mode waveguides in the mid-infrared, and secondly create the scattering centres required to extract the interferogram. All of the samples made in the context of this work were made in z-cut lithium niobate samples, using different technological combination: Direct Laser Writing for both the waveguides and the scattering centres, and Titane Diffusion for the waveguides combined with Focused Ion Beam for the scattering centres.

The DLW waveguides and centres were made by the ALF-USAL group in Salamanca, using the depressed index cladding technique. A femto-second laser is focused inside the sample, locally changing the refractive index of the material and creating so-called tracks. The waveguide is created by arranging these tracks in a crown-like structure, with the light that is confined inside this structure. The obtained refractive index change  $\Delta n$  is around  $10^{-3}$ , and the propagation losses  $\alpha$  around 2.2 dB/cm. DLW is a simple and fast technology, and it allows for 3D geometries and, in particular, buried waveguides.<sup>6</sup> Additionally, this technology allows to also create the scattering centres by focusing the laser this time at the surface of the sample, effectively writing tracks, or grooves, that will extract the light.

Titane diffused waveguides are made at FEMTO-ST, Besançon, through a lithographic process:<sup>7</sup> on chosen areas of the sample, titanium ions are diffused in Lithium Niobate, creating single-mode mid-infrared waveguides.<sup>8</sup> The obtained refractive index change  $\Delta n$  is at maximum around  $10^{-2}$ , and the propagation losses  $\alpha$  around 1.0 dB/cm. This technique allows to guide both the TE and TM polarisations with similar -relatively low-propagation losses. The following step is the use of a FIB to implement the scattering centres, also called grooves as the material is etched from the surface.

### 4. ANTENNAS

The angular divergence of the light radiated by the scattering centres may result in crosstalk, especially when considering classical mid-infrared detectors, where the active layer is usually buried under a substrate layer. Crosstalk, that is to say the leakage from the signal of one of the centres onto the signal from its neighbour, will result in a blend of the signals on the pixels, and an impossibility to reconstruct the interferogram or the spectrum of the source. To avoid this issue, the solution that has been proposed by Morand et al<sup>9</sup> is to implement several grooves per scattering centre, so as to create miniature diffraction gratings, allowing to reduce the angular divergence. These miniature diffraction gratings will from now on be called antennas.

The typical geometry for the antennas that were implemented is 5 grooves per scattering centre, all separated by  $1.6 \mu\text{m}$  ( $= \lambda/n_{eff}$ ). The optical set-up that was used for the characterisation of these antennas, in a Gabor-like configuration, requires to have the light injected on both side of the waveguide, and the radiation of the antennas imaged through a mid-infrared camera. The injection is made through the use of two converging lenses on each side of the sample, that collect the light coming from a monochromatic HeNe laser reflected onto a series of mirrors. The mirror on one side of the injection is movable, allowing for an external scan of the optical path difference, therefore creating an interferogram that will be sampled by the antennas. This interferogram, resulting from the interferences between the propagative and contra-propagative wave in the waveguide, can be expressed as:

$$I_T = I_1 + I_2 + 2 \cdot \sqrt{I_1 \cdot I_2} \cdot \cos\left(\frac{2\pi}{\lambda} \cdot \delta\right) \quad (4)$$

with  $I_1$  and  $I_2$  the flux from the propagative and contra-propagative waves, and  $\delta$  the optical path difference (OPD). The OPD corresponds to the geometrical path difference ( $x$ ) multiplied by the refractive index  $n$  of the medium in which this the geometric path is modified, and can correspond to the sum of several OPD modifications (for instance, external modulation  $\delta_{ext}$ , happening in air, combined with internal modulation  $\delta_{EO}$ , taking place inside the waveguide).

As the OPD is, in this case, modified through the movable mirror, we have:  $\delta = n_{air} \cdot x$ . As the cosine function is  $2\pi$  periodic, the period of the interferogram is expected to be  $\lambda$  in this case.

Finally, the radiated light is imaged on the camera with a converging lens (the final step for a complete SWIFTS

is to have the detector directly glued onto the sample, but it is not the case here). The image obtained on the camera will correspond to fig.2(bottom)\*:

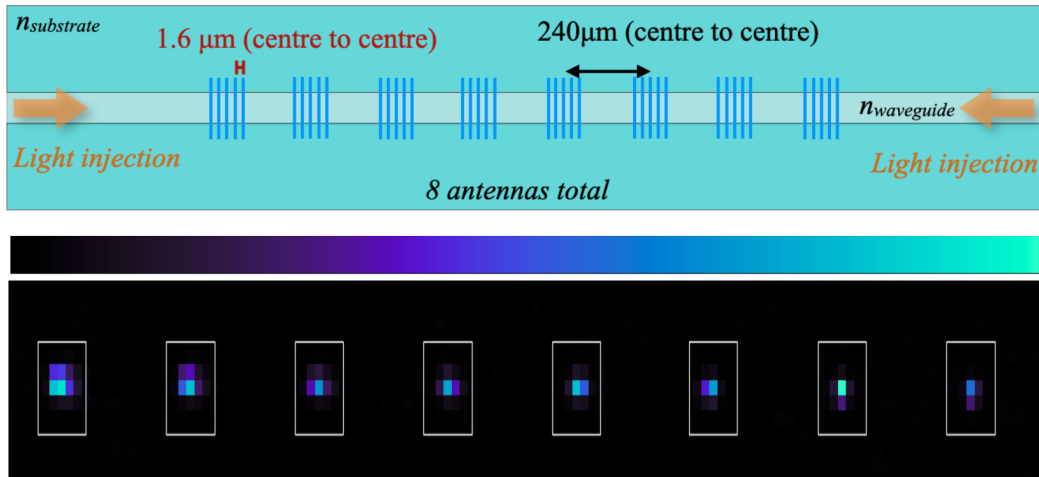


Figure 2: Schematics (top) of the geometry of the FIB antennas and radiated field (bottom) when the antennas are injected at  $3.39\mu\text{m}$ .

The movable mirror is then moved through the use of a motorised translation axis, allowing to vary the optical path difference over  $20\mu\text{m}$ , and the flux extracted by one antenna (for each of the technologies) is collected on the camera. Finally, the Fourier Transform of the interferogram is computed: fig.3 and fig.4.

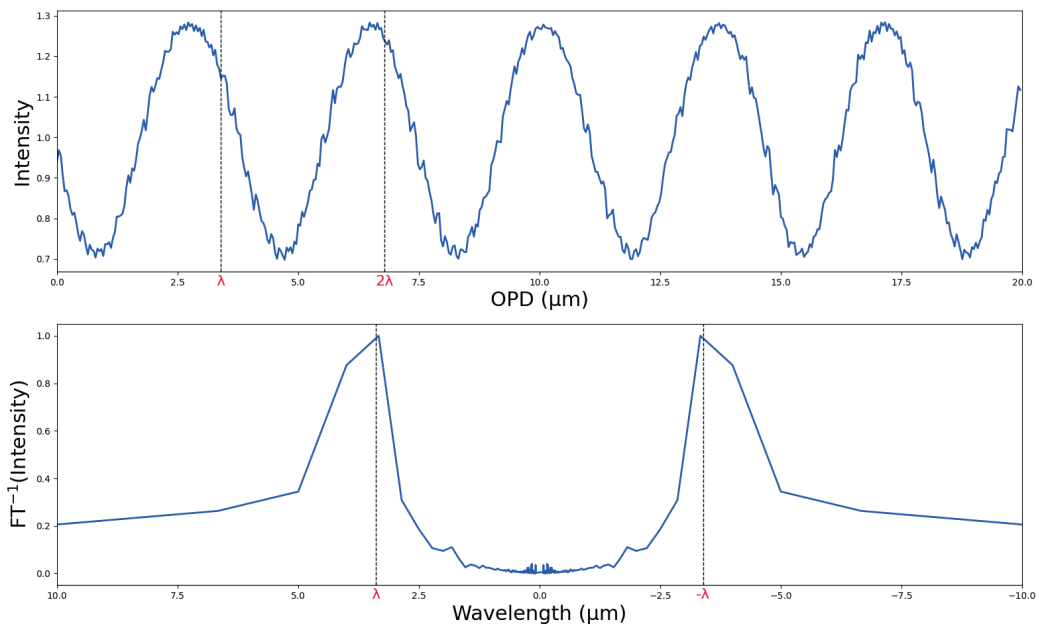


Figure 3: Direct Laser Written antenna: extracted interferogram (top) by one antenna and Fourier Transform of the interferogram (bottom).

For a reference, the value of the wavelength  $\lambda$  was plotted on each of the figures. It is visible that both the DLW and FIB antenna are extracting the interferogram with a period close to what was expected ( $\lambda$ ). The slight variation in the period of the interferogram might result from the fact that the movement induced by the

\*The python colormap of this figure and the following come from the cmasher catalogue<sup>10</sup>

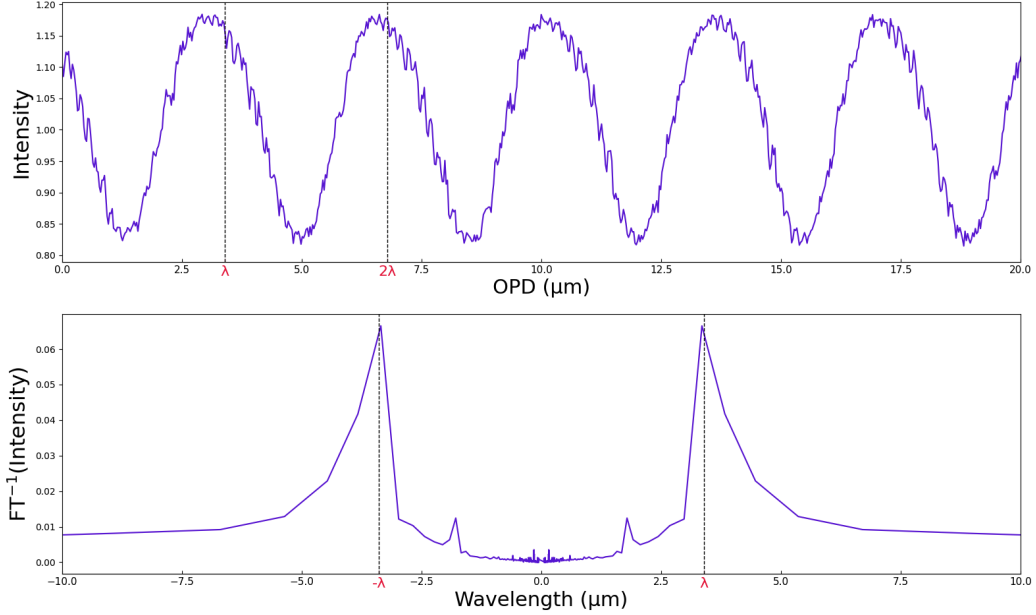


Figure 4: Focused Ion Beam antenna: extracted interferogram (top) by one antenna and Fourier Transform of the interferogram (bottom).

motorised platform might not be entirely smooth resulting in the optical path difference that might be slightly different than the theoretical one. Nonetheless, computing the Fourier Transform leads, in both cases, to a spectrum peaking at  $\lambda$  and  $-\lambda$ , as expected, showing that the antennas are working as expected.

## 5. CONCLUSION AND PERSPECTIVES

Mid-infrared antennas extracting an interferogram have been successfully implemented in the monochromatic case, with the aim to implement a SWIFTS Gabor configuration. These antennas have been, at the moment, studied individually, and the next step to implement a functional SWIFTS is to study the signal from all the antennas simultaneously. In the case of a laser, because of the high coherence length and cosine variation of the interferogram, a single antenna is sufficient to retrieve the wavelength of the source. However, when considering a polychromatic source, several antennas are required to sample the fringe packet. To do so, the pitch between the antennas should be small enough to ensure that the coherence length of the source is not smaller. As this reduction remains limited by the pixel pitch of the detectors, an external modulation similar to the one already implemented will allow to shift the fringe packet from one antenna to the other. Additionally,  $\text{LiNbO}_3$  was chosen for its electro-optic effect, that should be implemented in the near future through the connectorisation of the samples. This electro-optic effect will allow for an additional shift of the fringe packet, with an amplitude depending on the length of the electrodes, the width separating them, the applied voltage, etc. This effect remains of a much lower amplitude than the external modulation, and therefore also requires the antennas to be closer together. Finally, a higher number of antennas should be implemented, so as to increase the resolution. These results are paving the way for future technological iterations towards a miniature integrated mid-IR SWIFTS spectrometer.

## ACKNOWLEDGMENTS

IPAG Funding: Authors acknowledge the funding from Labex FOCUS (ANR-11-LABX-0013) and ASHRA (Action Spécifique Haute Résolution Angulaire) from INSU-CNRS.

USAL Funding: We acknowledge support from Ministerio de Ciencia e Innovación (PID2020-119818GB)

FEMTO-ST Funding: These works have been partially done within the French RENATECH network through its FEMTO-ST technological facility

## REFERENCES

- [1] Dorn, R. J., Bristow, P., Smoker, J. V., Rodler, F., Lavail, A., Accardo, M., van den Ancker, M., Baade, D., Baruffolo, A., Courtney-Barrer, B., Blanco, L., Brucalassi, A., Cumani, C., Follert, R., Haimerl, A., Hatzes, A., Haug, M., Heiter, U., Hinterschuster, R., Hubin, N., Ives, D. J., Jung, Y., Jones, M., Kaeuff, H. U., Kirchbauer, J. P., Klein, B., Kochukhov, O., Korhonen, H. H., Köhler, J., Lizon, J. L., Moins, C., Molina-Conde, I., Marquart, T., Neeser, M., Oliva, E., Pallanca, L., Pasquini, L., Paufique, J., Piskunov, N., Reiners, A., Schneller, D., Schmutzer, R., Seemann, U., Slumstrup, D., Smette, A., Stegmeier, J., Stempels, E., Tordo, S., Valenti, E., Valenzuela, J. J., Vernet, J., Vinther, J., and Wehrhahn, A., “CRIRES<sup>+</sup> on sky at the ESO Very Large Telescope. Observing the Universe at infrared wavelengths and high spectral resolution,” *Astronomy and Astrophysics* **671**, A24 (Mar. 2023).
- [2] Han, Z., Lin, P., Singh, V., Kimerling, L., Hu, J., Richardson, K., Agarwal, A., and Tan, D. T. H., “On-chip mid-infrared gas detection using chalcogenide glass waveguide,” *Applied Physics Letters* **108**, 141106 (04 2016).
- [3] Sun, H., Zhou, Y., and Li, L., “Miniature integrated spectrometers towards high-performance and cost-effective,” *Light: Science and Applications* **12**, 259 (Oct. 2023).
- [4] Le Coarer, E., Blaize, S., Benech, P., Stefanon, I., Morand, A., Lérondel, G., Leblond, G., Kern, P., Fedeli, J. M., and Royer, P., “Wavelength-scale stationary-wave integrated Fourier-transform spectrometry,” *Nature Photonics* **1**, 473–478 (Aug. 2007).
- [5] Bonduelle, M., Heras, I., Morand, A., Ulliac, G., Salut, R., Courjal, N., and Martin, G., “Near ir stationary wave fourier transform lambda meter in lithium niobate: multiplexing and improving optical sampling using spatially shifted nanogroove antenna,” *Appl. Opt.* **60**, D83–D92 (Jul 2021).
- [6] Nguyen, H.-D., Ródenas, A., de Aldana, J. R. V., Martín, G., Martínez, J., Aguiló, M., Pujol, M. C., and Díaz, F., “Low-loss 3d-laser-written mid-infrared linbo3 depressed-index cladding waveguides for both te and tm polarizations,” *Opt. Express* **25**, 3722–3736 (Feb 2017).
- [7] Heidmann, S., *Composants actifs en optique intégrée pour l’interférométrie stellaire dans le moyen infrarouge*, PhD thesis (2013). Thèse de doctorat dirigée par Benech, Pierre et Martin, Guillermo Optique et radiofréquence Grenoble 2013.
- [8] Courjal, N., Bernal, M.-P., Caspar, A., Ulliac, G., Bassignot, F., Gauthier-Manuel, L., and Suarez, M., [*Lithium Niobate Optical Waveguides and Microwaveguides*], IntechOpen, Rijeka (2018).
- [9] Morand, A., Heras, I., Ulliac, G., Coarer, E. L., Benech, P., Courjal, N., and Martin, G., “Improving the vertical radiation pattern issued from multiple nano-groove scattering centers acting as an antenna for future integrated optics fourier transform spectrometers in the near ir,” *Opt. Lett.* **44**, 542–545 (Feb 2019).
- [10] van der Velden, E., “Cmasher: Scientific colormaps for making accessible, informative and “cmashing” plots,” *Journal of Open Source Software* **5**, 2004 (Feb. 2020).